





# Promotion of Surgical Masks Antimicrobial Activity by Disinfection and Impregnation with Disinfectant Silver Nanoparticles

This article was published in the following Dove Press journal:  
*International Journal of Nanomedicine*

Benjamin Valdez-Salas <sup>1,2</sup>  
Ernesto Beltran-Partida <sup>1,2</sup>  
Nelson Cheng<sup>3</sup>  
Jorge Salvador-Carlos <sup>2</sup>  
Ernesto Alonso Valdez-Salas<sup>1</sup>  
Mario Curiel-Alvarez <sup>2</sup>  
Roberto Ibarra-Wiley<sup>2</sup>

<sup>1</sup>Laboratorio de Biología Molecular y Cáncer, Instituto de Ingeniería, Universidad Autónoma de Baja California, Mexicali, Baja California, Mexico; <sup>2</sup>Laboratorio de Corrosión y Materiales Avanzados, Instituto de Ingeniería, Universidad Autónoma de Baja California, Mexicali, Baja California, Mexico; <sup>3</sup>Magna International Pte Ltd, Singapore

**Background:** The COVID-19 pandemic is requesting highly effective protective personnel equipment, mainly for healthcare professionals. However, the current demand has exceeded the supply chain and, consequently, shortage of essential medical materials, such as surgical masks. Due to these alarming limitations, it is crucial to develop effective means of disinfection, reusing, and thereby applying antimicrobial shielding protection to the clinical supplies.

**Purpose:** Therefore, in this work, we developed a novel, economical, and straightforward approach to promote antimicrobial activity to surgical masks by impregnating silver nanoparticles (AgNPs).

**Methods:** Our strategy consisted of fabricating a new alcohol disinfectant formulation combining special surfactants and AgNPs, which is demonstrated to be extensively effective against a broad number of microbial surrogates of SARS-CoV-2.

**Results:** The present nano-formula reported a superior microbial reduction of 99.999% against a wide number of microorganisms. Furthermore, the enveloped H5N1 virus was wholly inactivated after 15 min of disinfection. Far more attractive, the current method for reusing surgical masks did not show outcomes of detrimental amendments, suggesting that the protocol does not alter the filtration effectiveness.

**Conclusion:** The nano-disinfectant provides a valuable strategy for effective decontamination, reuse, and even antimicrobial promotion to surgical masks for frontline clinical personnel.

**Keywords:** surgical mask, antimicrobial, SARS-CoV-2, nanobiotechnology, COVID-19, nanoparticles

## Introduction

The current alarming pandemic outbreak-associated to the new severe acute respiratory syndrome coronavirus 2 (SARS-CoV-2) results in coronavirus disease 2019 (COVID-19). In worst cases, the COVID-19 causes a severe respiratory disease, which could lead to the death of the patients.<sup>1</sup> Despite COVID-19 reported a lower fatality rate than other SARS-based coronaviruses,<sup>1</sup> the global impact regarding SARS-CoV-2 outstands in its exceptional ability to spread in different communities efficiently.<sup>2</sup> COVID-19 can lead patients to critical illness or, in the worst scenario, to severe secondary infections by opportunistic microorganisms,<sup>3-5</sup> even when using several protection schemes.<sup>6-8</sup> Furthermore, SARS-CoV-2 could be present in asymptomatic infected populations, but with a potential probability to transmit

Correspondence: Benjamin Valdez-Salas  
Tel/Fax +526865664154 Ext. 150  
Email berval@uabc.edu.mx

this viral agent.<sup>9</sup> Therefore, it is imperative to develop novel and outstanding protective strategies in order to reduce or avoid the transmission of this lethal infection disease.

A critical impact factor raised by the COVID-19 outbreak has been the international dwindled supply chain of protective masks and respirators,<sup>10</sup> which are fundamental to guard healthcare personal and the community. Moreover, the traditional manufacturer design of medical surgical masks is limited to a single use, which strongly influences the items reduced availability. Therefore, a contemporary challenge is an imperative mean to develop efficient decontamination and antimicrobial protocols that can be universally accessible. Several decontamination processes have been applied to reuse surgical masks and respirators, including UV germicidal irradiation, ethylene oxide, dry and steam sterilization in the autoclave, and ionized hydrogen peroxide.<sup>10–12</sup> However, it is important to highlight that those strategies are expensive; some require high-trained personnel, could result in detrimental effects to the masks and are not universally available in hospital installations as well for the social community. Consequently, an exemplary method is one that is simultaneously rigorous enough to afford maximal decontamination and yet provides antimicrobial activity. Interestingly, the textiles of the masks must be effectively decontaminated, incorporating human-safe antimicrobial agents, in order to avoid persistent microorganisms (eg, spore-forming bacteria) on the masks.<sup>10</sup> Nanotechnology has offered a substantial platform to design high surface-to-volume ratio configured materials capable of being fine-tuned for surface textiles, to achieve an optimal antimicrobial effectiveness. Moreover, nanotechnology could play a pivotal role in fighting against nosocomial microbial infections, such as SARS-CoV-2 and its surrogates. For example, AgNPs have been well documented to takedown different viruses by collapsing the envelopment integrity and disaggregation of the viral content,<sup>13</sup> a hallmarking advantage of AgNPs. Far more critical, metal-loaded nanocomposites into healthcare personnel polymeric equipment (eg, mouth masks) could effectively attenuate the viral viability and the prolonged SARS-CoV-2 persistence.<sup>14</sup> Furthermore, AgNPs have shown important applications in developing broad-spectrum antibacterial coatings,<sup>15</sup> anticancer strategies,<sup>16</sup> and biosensor systems.<sup>17</sup> Thus, an important and innovating option for the shielding of surgical mask fibers with advanced antimicrobial promotion is incorporating AgNPs

functionalized in a high-efficient disinfectant solution. Interestingly, in a previous study, Li et al fabricated surgical masks incorporated with top-down synthesized AgNPs.<sup>18</sup> The AgNPs modified surgical masks illustrated an effective antibacterial action. However, the authors reported that the AgNPs were present as a coating instead of an impregnation process, which can result in a detrimental skin cytotoxicity.<sup>18</sup> Considering the above-stated information, we rely on a promising strategy to formulate a broad-spectrum disinfectant, incorporated with antiviral-off metallic nanoparticles capable of bringing unique antimicrobial properties to the mask textile fibers with only an easy, accessible, and fast application. Therefore, we developed an alcohol-based disinfectant containing quaternary ammonium compounds and surfactants, as an exceptional platform for impregnating and retaining AgNPs in the surgical mask fibers.

This work aims to synthesize high-dispersed spherical 5–13 nm AgNPs by electrochemical dissolution of pure silver to formulate a novel broad-spectrum antimicrobial disinfectant. The nano-developed disinfectant was designed to uniformly coat hydrophobic surgical masks with AgNPs, promoting antimicrobial activity, as well as viral inactivation efficacy for healthcare protection. Our strategy further allows incorporating AgNPs to medical-grade textiles fibers of the surgical masks protecting against microbial penetration and adhesion. The present research has contributed as a novel, cost-effective, and accessible approach for the disinfection of medical textile mask materials to overcome the current limited supply chain that we are facing by the COVID-19. Far more attractive, the medical personnel of our institution and the school of medicine has been applying the present protocol.

## Materials and Methods

### Synthesis of Silver Nanoparticles

AgNPs were prepared by electrochemical synthesis following the method reported by Huang et al<sup>19</sup> and Khaydarov et al<sup>20</sup> with slight modifications. In brief, two high-purity silver rod electrodes of 2 mm diameter (99.999%, Sigma-Aldrich, St. Louis, MI, USA) were mechanically polished, washed with double distilled water, fitted using a polypropylene cover, vertically placed face-to-face at a distance of 1 cm, and submerged into a 1-L glass reactor. Next, 1 L of an aqueous solution containing 5 mg/mL PVP (K30, Sigma-Aldrich,

St. Louis, MI, USA) was deposited in the glass reactor and stirred with a PTFE stirrer controlled at 500 RPM at 65 °C. The electrolysis was adjusted to a constant voltage of 20 V, applied between the two electrodes simultaneously, for 1 h using a direct current power supply. The time for alternating polarities between the anode and the cathode was set to 1 min using an alternating polarity control. Finally, the resulting AgNPs solution was filtered (Whatman, No. 4) and stored in an amber glass container at room temperature (RT).

### Characterization of Silver Nanoparticles

#### High-Resolution Transmission Electron Microscopy (HR-TEM)

In order to analyze the structural morphology as well as the size and distribution of AgNPs we applied HR-TEM (JEM-2500SE, Jeol, Peabody, MD, USA). The AgNPs sample was placed drop-by-drop on carbon-coated copper grids and allowed to evaporate inside a controlled desiccator chamber, following a careful manipulation to avoid contamination. Next, the AgNPs were analyzed at 200 kV accelerating voltage to accomplish high-resolution imaging without any modifications, and the size distribution was calculated by counting nanoparticles ( $n=80$ ) present in the micrograph. The interplanar distances were measured using the Image J software (1.48v, NIH, USA), taking the scale bar as a measure reference from the crystal lattices detected by HR-TEM. The ring pattern of the selected area electron diffraction (SAED) is presented for the Ag crystallographic structure.

### Dynamic Light Scattering (DLS)

The size distribution (hydrodynamic diameter) and the Z-potential (ZP) of the AgNPs were studied using DLS. An aqueous suspension of AgNPs at pH 7.0 was filtered (Whatman, No. 4) and analyzed using a Nanotracs Wave II (Microtracs, North Wales, PA, USA) system with a delaying time of 30 s and a run time of 30 s at RT.

### Ultraviolet-Visible Spectroscopy (UV-Vis)

The UV-Vis analysis of the AgNPs suspension in deionized water was acquired using a UV/Vis spectrophotometer (UV-2600, Shimadzu, Japan), applying a scanning in the wavelength region of 300–600 nm with a resolution of 1 nm at RT.

### X-Ray Diffraction (XRD)

The pattern phases of the AgNPs were studied using a Bruker Advance D8 (Bruker, Billerica, Massachusetts, USA) diffractometer operated with a Cu  $K_{\alpha}$  radiation detector, a scatter screen height of 5 mm, a voltage of 30 kV and 30 mA. The scans were performed from 30° to 100° using a step size of 0.034° 2 $\theta$ .

### Disinfectant Formulation and Surgical Mask Disinfection by AgNPs

#### Impregnation

The present formulation represents the results of different chemicals tested for improving AgNPs incorporation and promoting antimicrobial activity into the surgical masks (part of the patent application No. 10202002135U). Therefore, we developed the disinfectant formulation by incorporating an aqueous solution of AgNPs (10% v/v) including 2% citric acid, into an ethanol aqueous solution (45% V/V ethyl alcohol) containing 0.03% triclosan (Sigma-Aldrich, St. Louis, MI, USA). Then, 0.2% of triton X-100 (Sigma-Aldrich, St. Louis, MI, USA) and 0.3% lauryl alcohol ethoxylate (LAE, 9 moles ethylene oxide; Sigma-Aldrich, St. Louis, MI, USA) were added and thoroughly homogenized. Next, different concentrations of benzalkonium chloride (BC, Sigma-Aldrich, St. Louis, MI, USA) were incorporated, as indicated in Table 1, to evaluate the effect in the antimicrobial activity. The corresponding final volume was completed with superoxidized water solution (Microdacyn 60<sup>®</sup>, Oculus Technologies, Guadalajara, México). In order to disinfect, impregnate AgNPs and promote antimicrobial activity to the surgical mask, we dipped the textile material into the disinfectant for 5 min at RT and dried in a controlled desiccator until complete dryness.

### Fourier-Transformed Infrared Spectroscopy (FT-IR) of the AgNPs-Impregnated Surgical Masks

To explore the chemical groups' modifications followed by impregnation with AgNPs, an attenuated total reflection (ATR) FT-IR spectrometer (Frontier, Perkin Elmer, USA) was used. The spectra were acquired at a resolution of 1  $\text{cm}^{-1}$  applying a scanning range of 400–4000  $\text{cm}^{-1}$ .

**Table 1** Formulated Disinfectants for Antimicrobial Activity of Surgical Mask Fibers

	Formulation a	Formulation b	Formulation c	Formulation d
BC	0	0.05	0.1	0.2
Ethanol-water 45% V/V	85	85	85	85
Triclosan	0.03	0.03	0.03	0.03
AgNPs	10	10	10	10
LAE	0.3	0.3	0.3	0.3
Triton X-100	0.2	0.2	0.2	0.2
Citric acid	2	2	2	2
Microdacyn 60 <sup>®</sup>	To complete 100%			

**Abbreviations:** BC, benzalkonium chloride; AgNPs, silver nanoparticles; LAE, lauryl alcohol ethoxylate. Values are represented in percentage (%).

## Field-Emission Scanning Electron Microscopy (FE-SEM) of the AgNPs-Impregnated Surgical Masks

The impregnation of AgNPs into the surgical mask fibers was characterized using FE-SEM (LYRA 3, Tescan, Brno, Czech Republic), at 10 kV accelerating voltage with a backscattered electron detector. The surgical masks previously dipped in the disinfectant formulation containing AgNPs, and dried at RT in a controlled desiccator, were sampled on a double-sided adhesive carbon conductive tape before FE-SEM analysis.

## Energy-Dispersive X-Ray Spectroscopy (EDX) of the AgNPs-Impregnated Surgical Masks

The chemical analysis was carried out by EDX (XFlash 6130 Bruker, Billerica, Massachusetts, USA) coupled to the FE-SEM, at 10 kV with a large spot size to adjust a suitable count rate per second for spectrum collection.<sup>21</sup>

## Water Contact Angle (WCA) of the Surgical Masks

The WCA of the experimental surgical masks was evaluated by depositing a 5  $\mu$ L droplet of deionized water at 25 $^{\circ}$  C and 45% relative humidity for 0s, 5s, and 10s.<sup>22,23</sup> An automatized tensiometer (Theta Attension; Biolin Scientific, Gothenburg, Sweden) equipped with an X-Y syringe and a high-performance CCD camera was used to capture high-resolution images. The WCA values were quantified using the ONE Attension software (Biolin

Scientific, Gothenburg, Sweden) which enables a highly precise analysis of the two angles of the drop.<sup>21</sup>

## Microbial Culture

Pathogenic models of nosocomial microbial infectious diseases strongly associated with secondary infections followed COVID-19 [3, 4] were used as supporting surrogates of SARS-CoV-2 for antimicrobial activity. The Gram-negative models tested were *Escherichia coli* (*E. coli*, ATCC 25922), *Klebsiella pneumoniae* (*K. pneumoniae*, ATCC 13883) and *Pseudomonas aeruginosa* (*P. aeruginosa*, ATCC 27853). The Gram-positive bacterium was *Staphylococcus aureus* (*S. aureus*, ATCC 25923). A yeast infection model was *Candida albicans* (*C. albicans*), isolated from an oral denture candidiasis patient as previously described.<sup>21,24</sup> In order to prepare the working microbial cultures, discrete colonies of freshly grown cells were inoculated each separately into newly prepared Tryptic soy broth (TSB; Becton Dickinson, Sparks, MD, USA) for bacteria and potato dextrose broth (PDB; Becton Dickinson, Sparks, MD, USA) for *C. albicans*. Furthermore, each inoculum was diluted in the corresponding newly broth to approximately  $1 \times 10^7$  colony-forming units (CFU)/mL, which was used as microbial concentration for the antimicrobial studies.<sup>25</sup>

## Antimicrobial Activity of the Disinfectants by Recovery Media Evaluation

For the evaluation of the antimicrobial activity of the disinfectant formulation at different BC concentrations, we performed the neutralization and recovery of viable

cells technique reported by Dey and Engley with slight modifications.<sup>26</sup> One milliliter of the each formulated disinfectant (Table 1) was deposited into 8.9 mL of Dey and Engley (D/E) neutralizing broth (Sigma-Aldrich, St. Louis, MI, USA), mixed thoroughly and incubated for 30 min at RT. Next, the mixture was inoculated with 0.1 mL of each working microbial culture in separate and incubated at 37°C for 48 h. Afterwards, each culture tube was carefully shaken for 15s, 0.1 mL of each culture mixture was plated on to a fresh D/E agar (Sigma-Aldrich, St. Louis, MI, USA) plate. Each microbial evaluation was incubated at 37°C for 48h. After incubation, the recovered organism was counted and expressed as log<sub>10</sub> of CFU/mL.

### Microbial Challenge Study

The microbial challenge was carried out following the Mexican Official Norm guidelines for germicidal testing NMX-BB-040-SCFI-1999.<sup>27</sup> This norm indicates that any germicide must reduce the initial viable microbial load of *E. coli* and *S. aureus* by 99.999% in 30 s of exposure, at the recommended dose. For the present study, we used the working microbial cultures, as stated above. Initially, 1 mL of each microbial suspension was transferred to 9 mL of the disinfectant formula containing 0.2% BC, using a sterile pipette. Consecutively, a calibrated time was immediately adjusted and initiated at different experimental times (0.5, 1.0, 5.0, and 10.0 min). Next, at the corresponding time points, each suspension was gently homogenized, and 1 mL of culture mixture was diluted with 9 mL of D/E neutralizing broth. Subsequently, 1 mL of the neutralized solution was plated and spread on tryptic soy agar (TSA; Becton Dickinson, Sparks, MD, USA) plates. Two plates per condition were used and incubated at 35°C for 48 h, in aerobic conditions. The resulting number of growing colonies on each plate was counted, and the reduction percentage was calculated using the initial microbial load. On the other hand, positive controls for each microorganism were tested in parallel using deionized water. The negative controls were the commercially available disinfectants Lysol<sup>®</sup> (Benckiser, México) and Dermoclean<sup>®</sup> (D.C.; Degasa, México) following the manufacturer's recommendations.

### Agar-Diffusion Test of the Formulated Disinfectants

The antimicrobial diffusion activity of the formulated disinfectants was evaluated applying the agar diffusion

test.<sup>26</sup> Initially, 0.1 mL of separate test organisms were cultured on TSA plates (25 mL of liquid TSA per 100 mm petri dish). After 30 min, we generated 3 holes of 7 mm diameter and 4 mm depth per dish. Next, 50 µL of the corresponding testing disinfectant was loaded separately for each organism and incubated at 37°C for 24h. The resulting inhibition zones (IZ) were measured using an electronic digital caliper and digitalized on a dark field colony counter (Reichert, NY, NY, USA).

### Agar-Diffusion Test of the AgNPs-Impregnated Surgical Masks

To perform the diffusion test from AgNPs-impregnated surgical masks, we soaked 0.5 cm<sup>2</sup> of textile materials into 10 mL disinfectant formula containing 0.2% BC and dried at RT. Next, 0.1 mL of each freshly prepared working organism was spread onto TSA plates. After 1h, three pieces of impregnated surgical masks were placed on the TSA and incubated at 37°C for 24 h.<sup>26</sup> The resulting IZ were measured using an electronic digital caliper and digitalized on a dark field colony counter (Reichert, NY, NY, USA).

### Antiviral Activity of the Disinfectant

We used the enveloped H5N1 avian influenza virus model, as a viral surrogate of coronavirus, following the procedures described elsewhere,<sup>28</sup> with slight modifications. A viral stock at 10<sup>7.7</sup> egg infectious dose 50 (EID 50) was propagated in the allantoic cavities of embryonated hen's eggs. Next, a diluted virus working culture (10<sup>5.0</sup> EID 50) was prepared in PBS containing 500 units/mL penicillin (Sigma-Aldrich, St. Louis, MI, USA), 500 µg/mL streptomycin (Sigma-Aldrich, St. Louis, MI, USA), and 1.25 µg/mL amphotericin B (Sigma-Aldrich, St. Louis, MI, USA). Then, 250 µL of the diluted virus was mixed with 500 µL of a 1:1 dilution of the 0.2% B. C. formulated disinfectant (in sterile distilled water) and incubated for 15 min at 37°C. Then, 200 µL of the disinfectant mixture was injected into the allantoic cavities of three 11-day-old embryonated hen's eggs and incubated at 37°C till the embryos die. The allantoic fluid was aseptically separated and analyzed using a rapid hemagglutination test for avian influenza. The presence of hemagglutination was considered positive for H5N1 virus survival.

## Statistical Analysis

Data analysis was performed using the results of three independent studies elaborated each in triplicate. The numerical information was expressed as the mean  $\pm$  standard deviation (SD) and analyzed using GraphPad Prism 7 (GraphPad Software Inc., San Diego, CA, USA). The significance of differences was tested using one-way analysis of variance (ANOVA) followed by Tukey's multiple comparison tests, and Student *t*-Test when appropriate.<sup>29</sup> A  $P < 0.05$  was considered statistically significant.

## Results and Discussion

The current outbreak-associated with the COVID-19 is demanding novel strategies which generate solutions to assess the shortage of surgical masks and even different medical textile materials.<sup>2</sup> Our main objective was to develop a broad-spectrum disinfectant with high antimicrobial AgNPs for surgical masks shielding, which could be

accessible and easy to use for our medical staff and the population. Thus, we synthesized AgNPs using a simple electrochemical etching method. Initially, the AgNPs presented a spherical-like morphology, that were highly mono-dispersed (Figures 1A and S1), as expected.<sup>19</sup> The HR-TEM characterization suggested that sphere NPs (Figure 1B) presented a detailed interplanar space of 2.33 Å (Figure 1C). Thus, suggesting the (111) crystallographic plane strongly referred to that of Ag<sup>0</sup> species are composing the AgNPs.<sup>30</sup> This interesting observation matches to those observed in our SAED analysis (Figure 1D) and agrees with previous reports of AgNPs.<sup>30,31</sup> Moreover, according to the TEM results, the size distribution of the AgNPs is 13.2 $\pm$ 4 nm showing a narrow size curve, as indicated in Figure 1E. Furthermore, the surface plasmon resonance (SPR) of AgNPs was 405 nm (Figure 1F), further following a narrow peak-valley behavior advising a monodispersity distribution<sup>31</sup> and part of the metallic state of Ag<sup>0</sup>

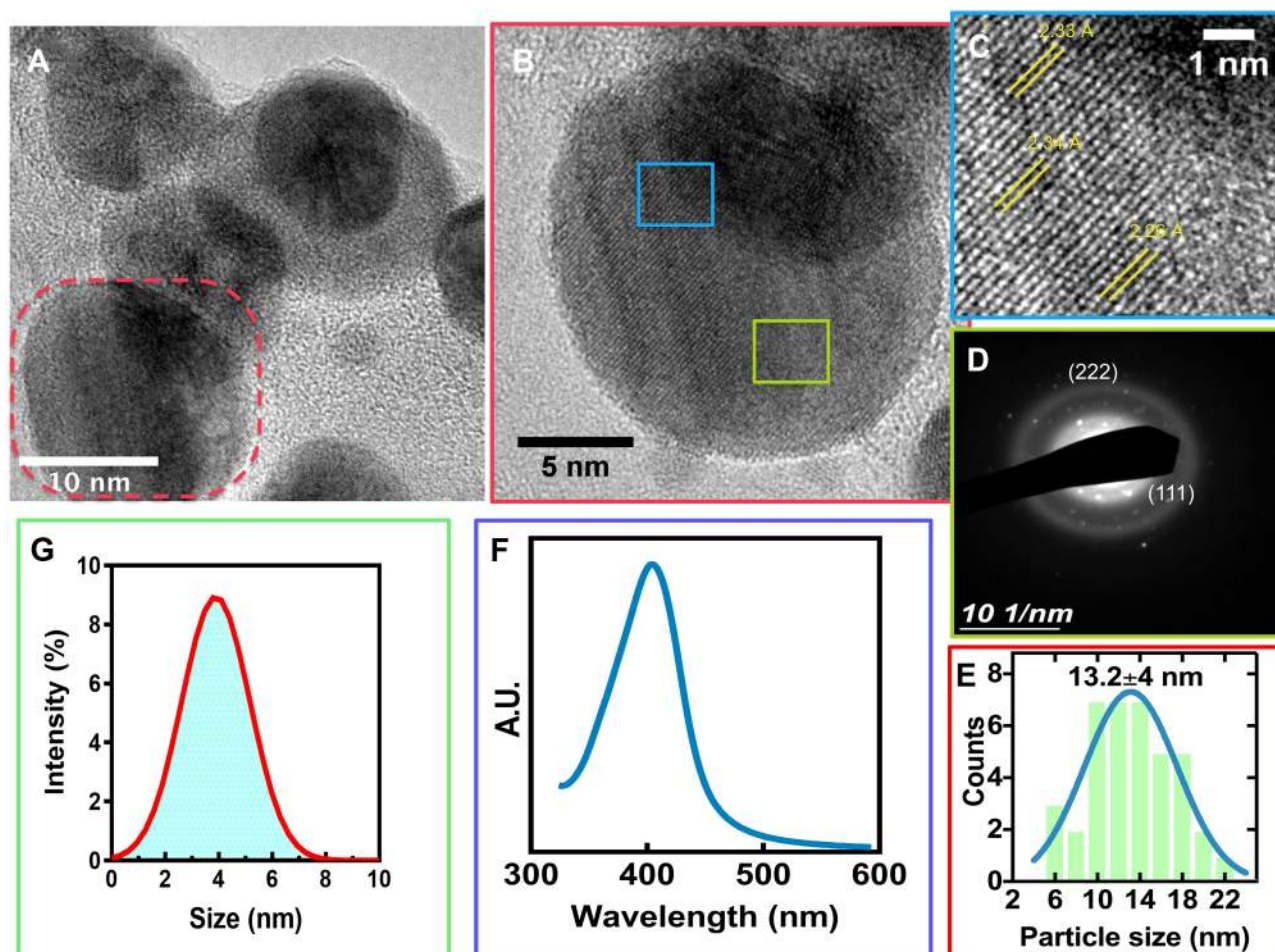


**Figure 1** Physicochemical characterization of the AgNPs. (A) HR-TEM micrograph illustrating the morphology of AgNPs, the red dotted area illustrates a magnification represented in (B). (C) interplanar distances of the AgNPs. (D) SAED patterns of AgNPs. (E) Particle size distribution by HR-TEM. (F) UV-Vis spectrum of the AgNPs. (G) DLS analysis of AgNPs.

species,<sup>20</sup> in accordance to Figure 1E and D. The DLS proposed that the AgNPs in solution showed a small diameter of 3.5 nm with a stable ZP of  $-112.2$  mV. The present results point toward that the electrolysis technique designed for AgNPs fabrication initially involves the dissolution of the Ag rod by losing electrons to form  $\text{Ag}^+$ , thus far, acting as a sacrificial anode.<sup>20</sup> Then,  $\text{Ag}^+$  species could be reduced on the cathode, generating zero-valent  $\text{Ag}^0$  and by van der Waals forces, the  $\text{Ag}^0$  can nucleate and grow to AgNPs.<sup>19</sup> In order to control the nucleation process, we included PVP in the synthetic protocol. The asymmetric chemical structure of the pyrrolidone group allows an excellent dispersant ability to control the nucleation of AgNPs<sup>32</sup> and protects of extensive NPs agglomeration.

A critical issue for promoting antimicrobial effectiveness to clinical surgical masks is in an accurate, controlled, and dispersed deposition of AgNPs. Thus, we applied FE-SEM

on the experimental masks, discovering a well-homogenized AgNPs distribution with slight conglomeration of AgNPs (Figure 2A). Interestingly, the as-observed agglomeration zones may promote a better integration of the fibers with  $\text{Ag}^0$  species (as suggested by SAED), which inversely can be translated in increased antimicrobial action (as discussed later). Moreover, the high-zoom presented in Figure 2B and C showed consistent outcomes of AgNPs coating over the broad surfaces of the fibers, and a dispersed deposition of smaller AgNPs as illustrated in Figure 2D (see insets). Interestingly, a nanoagglomeration phenomenon could be detected because of the drying effect applied to the coated fiber. Importantly, it has been wide documented that the stability of colloidal metallic nanoparticles (eg, AgNPs) are primarily dependent of the solvent suspension, the ionic strength, the pH, and the type of capping agent.<sup>33</sup> Those factors can provide steric and/or electrostatic repulsion,

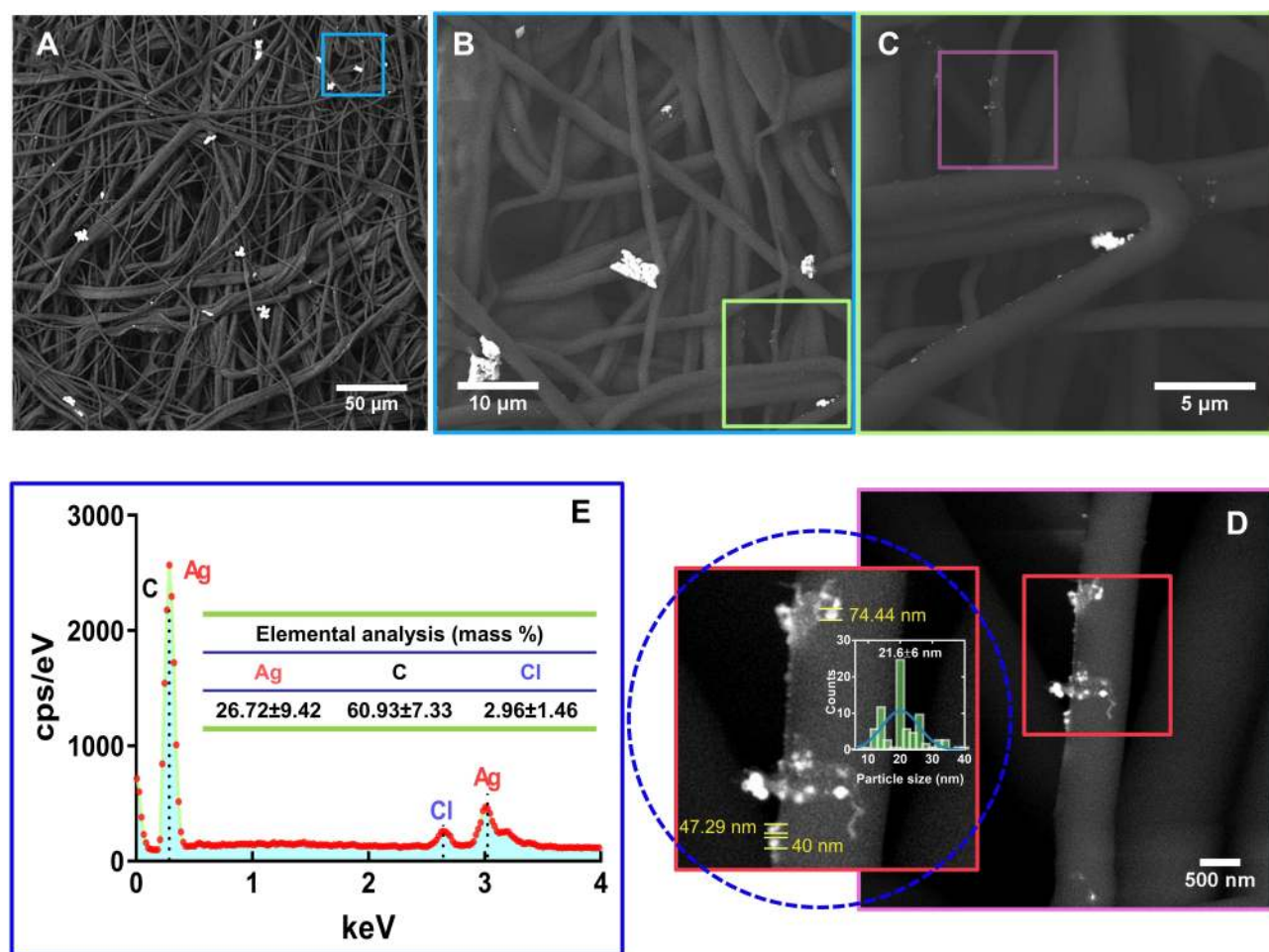


**Figure 2** Physicochemical characterization of surgical mask fibers impregnated with AgNPs. (A) FE-SEM micrograph of incorporated AgNPs onto the fibers. (B) AgNPs deposition over the fibers at higher magnification. (C) High zoom illustration of the AgNPs deposition on the fibers. (D) Surface-contact interaction behavior between AgNPs and fiber surface, illustrating a homogenous NPs deposition. (E) EDX.

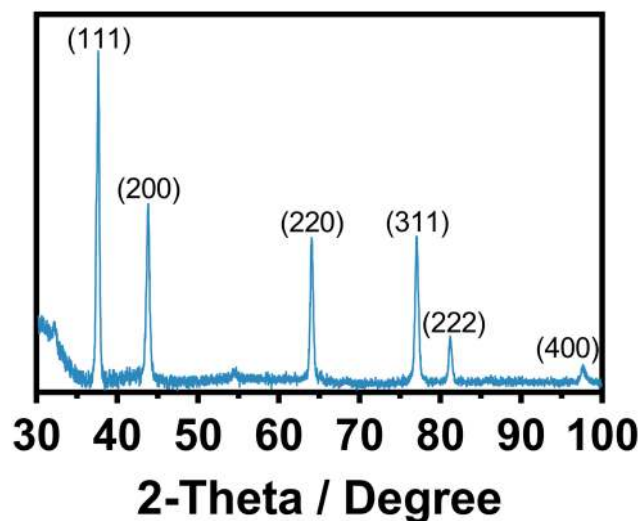


**Figure 3** XRD patterns showing the face orientation of the AgNPs.

which substantially influence in preventing AgNPs agglomeration. However, when AgNPs are submitted to drying processes, most of the above-mentioned physicochemical parameters are avoided; therefore, AgNPs could not effort the required dispersing repulsive charges. Thus consequently, AgNPs become extremely susceptible to agglomeration and deposition.<sup>34</sup> In a previous study, I. Osório et al deposited AgNPs on cotton fibers, thus resulting in AgNPs deposition being dependent on the concentration.<sup>35</sup> However, the electrostatic energy provided by the fiber surfaces could increase the aggregation rate by declining the electrostatic energy barrier to conduct AgNPs aggregations.<sup>33,36</sup> Therefore, our results suggested that the AgNPs distribution over the surgical mask were of  $21.6 \pm 6$  nm. It is important to highlight that our present study showed an efficient impregnation of AgNPs among the surface fibers, without the formation of a thick NPs coating that could raise detrimental alterations to the textile fibers. On the other hand, the EDX analysis illustrated the presence of silver element ( $26.72 \pm 9.42\%$ ) over the textile fibers (Figure 2E), far more supporting the presence of AgNPs. Our results are in accordance with Hiragond et al, which suggested the deposition of 9–14 nm AgNPs on the textile surgical mask surface.<sup>37</sup> The authors indicated an elemental Ag concentration of 12.93% by EDX, almost half of those observed here. This interesting behavior can be explained by considering two essential strategies: 1) AgNPs developed by chemical reduction vs our electrochemical AgNPs and 2) the coating of as-prepared AgNPs versus those formerly impregnated in our disinfectant containing surfactants. Surgical mask fibers are intended to

be hydrophobic, thus, surfactants are special chemical compounds that can act as a platform to reduce the surface tension between a liquid and a solid surface.<sup>38</sup> Therefore, the application of triton X-100, LAE, and BC (quaternary ammonium base) will serve as a cornerstone for efficient impregnation and dispersion of AgNPs into the fibers,<sup>39,40</sup> without developing a cracking coating, as compared to those previously reported.<sup>37</sup> On the other hand, the electrochemical synthetic pathway results in the formation of mainly  $\text{Ag}^0$  (Figure 1D), enabling efficient incorporation of  $\text{Ag}^0/\text{Ag}^+$ . Consequently, the related protocol could exacerbate the formation of a rougher, thicker, and non-homogenous Ag layer that could detracts the mask properties. On the other hand, the XRD analysis of the AgNPs Figure 3 showed significant peaks corresponding to the centered cubic phase of  $\text{Ag}^0$ . The peaks were assigned at  $2\theta$  of  $37.61^\circ$  (111),  $43.79^\circ$  (200),  $64.06^\circ$  (220),  $77.05^\circ$  (311),  $81.19^\circ$  (222) and  $97.7^\circ$  (400) indicating, the classical crystalline plane of Ag. The diffraction patterns are in agreement with the JCPDS 04–0783, our SAED results (Figure 1D), and previous works.<sup>41</sup>

As represented in Figure 4, we did not detect significant chemical shifting after incorporating the AgNPs with the surfactants at different BC concentrations. However, the FT-IR illustrated that the impregnation process does not alter the chemical configuration of the mask textiles, as we only identify some variable intensities. Interestingly, a decreased peak behavior was detected in the region of  $1300\text{--}1100\text{ cm}^{-1}$ , suggesting a reduced C-O stretching bonding by the increment in the BC and better incorporation of the  $\text{Ag}^0$  species. Moreover, the heightened

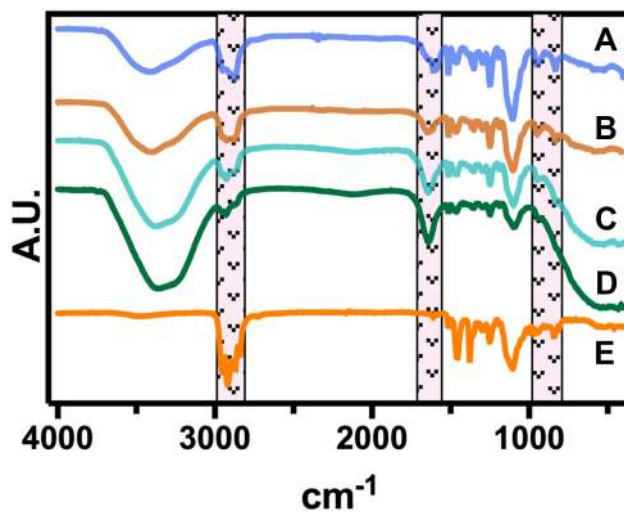


**Figure 4** FTIR spectroscopy of the surgical mask fibers with AgNPs at different BC concentrations. (a) 0%, (b) 0.05%, (c) 0.1%, (d) 0.2% and (e) without surfactants.



concentration of BC correlates to the aromatic C–C vibration detected in the region of  $1600\text{ cm}^{-1}$ , proposing that the quaternary ammonium has been incorporated. Similarly, the AgNPs did not show any significant chemical shifting, only highlighting the absence of the –OH in the region of  $3500\text{--}3200\text{ cm}^{-1}$ . Far more attractive, the classical C–H stretching in the region of  $3000\text{--}2800\text{ cm}^{-1}$  were almost similar between the different treatments. Taking together the FT-IR and FE-SEM analyses, we can hypothesize that the structural properties of the textile masks are not degraded after disinfectant incorporation.<sup>42</sup> Far more attractive, Fisher et al studied the filtration effectiveness of N95 respirators decontaminated in several cycles of 70% ethanol immersions.<sup>43</sup> The results indicated that 70% ethanol disinfection did not significantly alter the filtration efficiency of the respirator. Thus, affording, a significant disinfection rate of SARS-CoV-2 for the ethanol solution. The front-line shreds of evidence provided by Liao et al showed that surgical mask fibers disinfected using extremely high temperatures under different humidity conditions do not compromise the filtration efficiency.<sup>44</sup> The authors discovered that almost 20 cycles of  $100^\circ\text{C}$  for 5 min were not enough to alter the pressure drop of the textile fibers.<sup>44</sup> Moreover, in a previous study Cui et al proposed that transparent nanofiber membranes of polyvinyl alcohol and sodium lignosulfonate could adequately filtrate particle matter of 2.5, even after 10 cycles of circulation filtration.<sup>45</sup> Far more important, we applied WCA over a 0.2% BC-impregnated mask and a control non-treated mask (Figure S2). The results advocated that the impregnation process does not promote a significant water uptake behavior, as the droplets' morphologies were similar (Figure S2A). On the other hand, the quantitative analysis did not indicate significant differences, further supporting a relevant hydrophobicity performance after the impregnation process (Figure S2B), thus in accordance to previous works.<sup>22,23</sup> Hence, we suggest that the filtration capability by our decontamination process is not negatively compromised, as we did not detect morphological, chemical and wetting alterations. However, we recommend a future evaluation of aerosol filtration performance after several disinfecting cycles and mechanical test integrities.

The current SARS-CoV-2 outbreak has shown an impressive survival capability under different environmental conditions and surface materials. Moreover, recent studies have shown that SARS-CoV-2 can present a long half-life capability on common stainless steel and plastic

surfaces.<sup>46</sup> Furthermore, Chan et al suggested that SARS-CoV-2 conserve stable viability for 3–5 days under dry conditions, and as far as 7 days in solution conditions ( $20\text{--}25^\circ\text{C}$ ).<sup>47</sup> Additionally, this research group described that SARS-CoV-2 could stay active for up to 14 days at  $4^\circ\text{C}$ , which indicates the prolonged viral capability to spread by contact with contaminated surfaces. Despite the noteworthy survival ability of this pathogen, it has been described that can be inactivated and eliminated using several disinfectants, such as those based on alcohol formulas.<sup>48</sup> Therefore, we designed a new disinfectant based on 45% ethanol solution with protein destabilizing surfactants, superoxidized water, triclosan and fortified with AgNPs, for surgical mask disinfection and shielding. Applying the recovery media technique proposed by Dey and Engley,<sup>26</sup> we detected that the BC. And, 0.2% formula completely eradicated the growing ability of Gram (+), and (–) bacteria (Figure 5). Moreover, this trend was also detected for *C. albicans*, an opportunistic yeast capable to develop nosocomial infections.<sup>21</sup> Interestingly, the commercially acceptable disinfectant products showed similar outcome of disinfection; however, they diverge from AgNPs. It is important to highlight that the applied recovery media strategy essentially counteract the inhibitory action of the above selected chemicals, thus allowing the direct interaction with AgNPs (data not shown). Indicating that our new designed disinfectant is capable to eliminate an important number of microorganism associated with COVID-19 related secondary infections.<sup>3,4</sup> A cornerstone for disinfectant effectiveness consists in a comprehensive reduction viability of 99.999% for up to 30 s. On this basis, we applied the microbial challenge test for 0.2% BC formulation, resulting in 99.999% reduction for the evaluated microorganisms.

In order to analyze the competing antimicrobial action between the disinfectants, we used the agar diffusion test (Figure 6). Interestingly, the Gram (–) bacterial models showed among comparable outcomes of antibacterial activity. Furthermore, the Gram (+) model indicated a similar behavior as those of Gram (–), which suggested remarked checkpoints of dose-dependent manner, as advocated by the increasing BC concentrations. However, in the *E. coli* and *C. albicans* models, we observed a superior action for our disinfectant even than those of the Lysol product (Figure 6). Taking together the results presented in Figures 5 and 6, we can highlight that these used microorganisms can be considered as effective surrogates of SARS-CoV-2. Bacteria, and of particular interest fungi, present a more complex structural

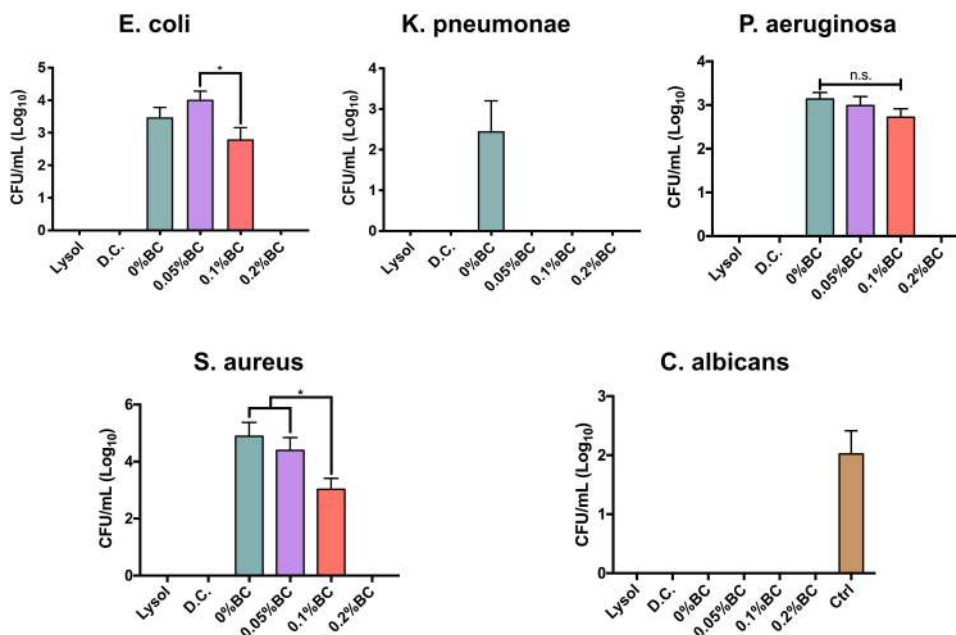


**Figure 5** Broad-spectrum microbial viability assessment of the formulated disinfectants containing AgNPs and the corresponding commercial controls. The \* indicates significant differences. n.s. shows non-significant changes.

**Abbreviations:** D.C., Dermocleen®; BC, benzalkonium chloride.

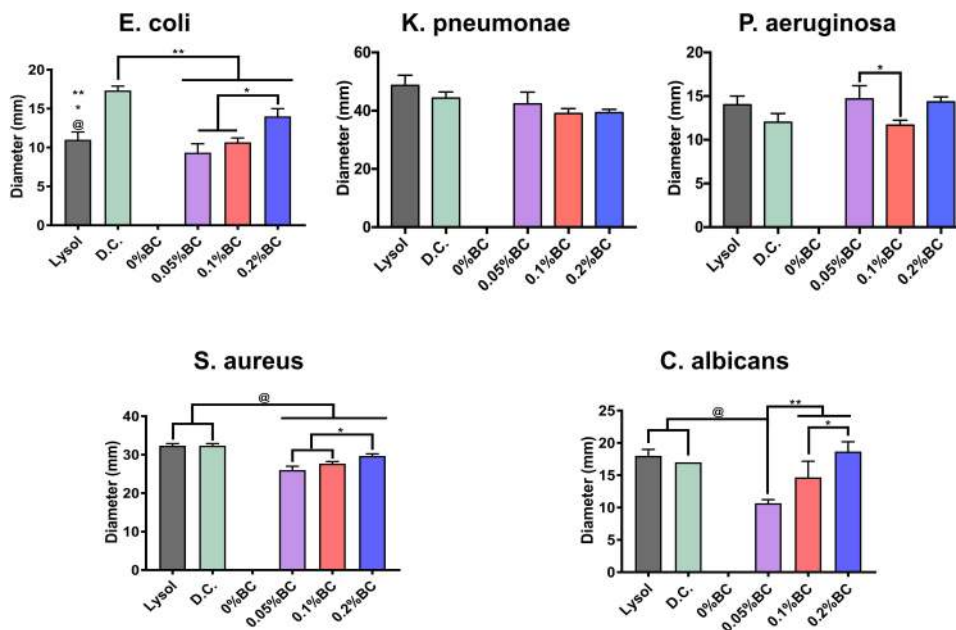


**Figure 6** Antimicrobial activity of the formulated disinfectants with AgNPs including the commercial controls. The \*, \*\* and @ indicates significant differences among the experimental formulations.

**Abbreviations:** D.C., Dermocleen®; BC, benzalkonium chloride.

physiology, which turned them less susceptible to chemical microbicidal processes than enveloped viruses, such as SARS-CoV-2.<sup>10</sup> On the other hand, a featured trend of antimicrobial action was detected for the striking broad-spectrum generated by the AgNPs-impregnated surgical

mask textiles (Figure 7). As allocated for the textiles, the microbial models were extensively sensitive to direct contact evaluation. Concomitantly, the fungi organism presented an outstanding antifungal action, further compared to inferior complex bacterial models. Our results are in accordance with

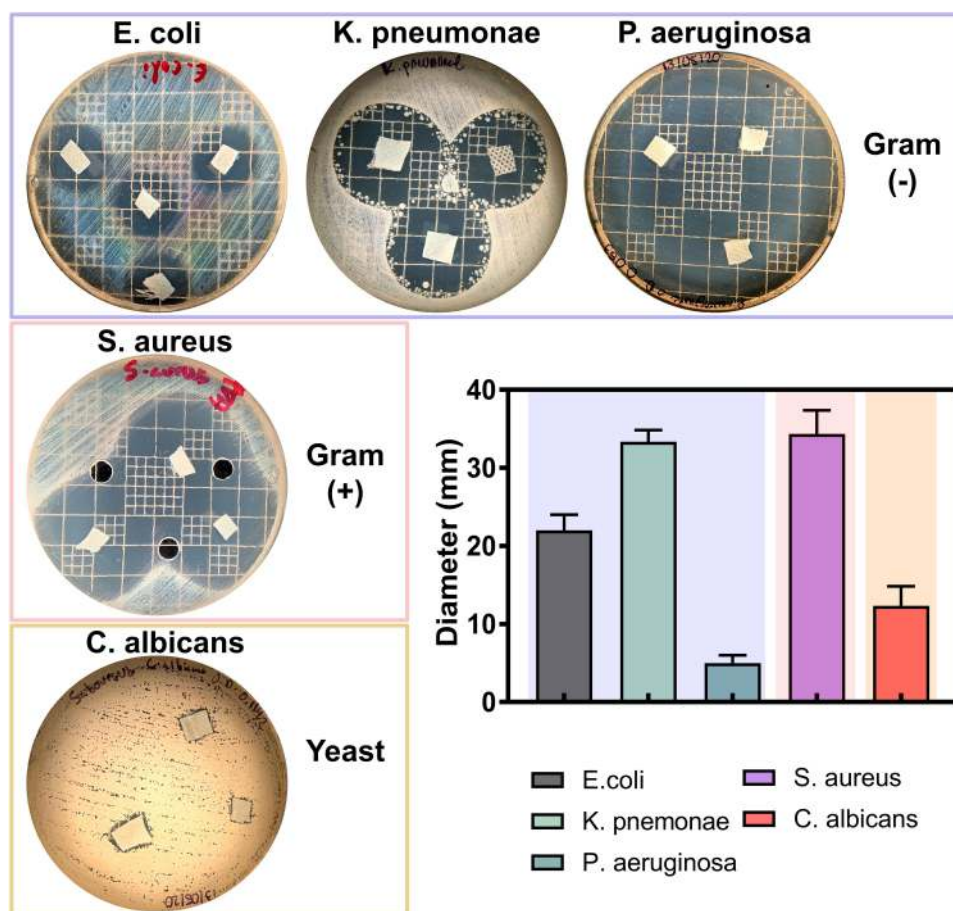


**Figure 7** Antimicrobial activity of the impregnated surgical masks with 0.2% BC formulation containing AgNPs.  
**Abbreviations:** D.C., Dermocleen®; BC, benzalkonium chloride.

a previous work of antibacterial surgical mask developed with AgNPs and TiO<sub>2</sub>NPs.<sup>18</sup> The authors synthesized the metallic NPs using a top-down pulverization approach, which were coated using a textile rolling machine. Moreover, Hiragond et al used colloidal AgNPs by chemical reduction and generated a thick silver coating on surgical mask fibers.<sup>37</sup> The coating resulted in a promoted antibacterial action against *S. aureus* and *E. coli*. However, the application of those coating strategies could lead to an obliteration of the AgNPs, due to a most direct contact with the human skin and bulk delivery of silver.<sup>18,49</sup> Similarly, a detrimental mask integrity, thus decreasing the filtration efficiency. Hence, a current trend is selecting an impregnation strategy that may improve the incorporation of the AgNPs into the textiles,<sup>49</sup> resulting in an improved antimicrobial and viral-off action due to the slow and continuous release of silver, as observed here. Importantly, our novel strategy supported a distributed incorporation of AgNPs among the textile fibers, which may strongly decrease the AgNPs leakage into the dermal contacting tissue.<sup>50</sup> Interestingly, AshaRani

et al suggested that starch-coated AgNPs (6–20 nm) could induce alterations in the morphology, viability, metabolic activity, and reactive oxygen species activation in human fibroblasts.<sup>51</sup> However, the authors indicated that its required concentrations higher than 50 µg/mL and direct contact periods longer than 48h to reduce almost 20% of the ATP activity.<sup>51</sup> Furthermore, a previous study of commercially available spherical 20 nm AgNPs (≈ 7 ppm) proposing 80% reduction in the L929 mouse fibroblasts metabolic activity after 24h of continuous contact.<sup>52</sup> On the other hand, it has been documented that AgNPs could exacerbate a given ecological impact, principally when infused into soil and water systems.<sup>53</sup> Nonetheless, despite the controversial effect of AgNPs on microbiota and plant systems, studies have indicated that long-lasting AgNPs regimens are mainly linked to overcoming toxic and imbalanced ecosystem impairments.<sup>54</sup> Therefore, it is substantial to highlight that the AgNPs concentration used for the impregnation formulation is several folds lower than those previously reported of harmful effects. Further proposing that our formulation is

ecofriendly and the level of AgNPs used is tolerable for mammalian cells. Hence, supporting that the impregnation process could decrease the AgNPs leakage could provide a future alternative for recycling surgical masks, reducing the environmental pollution.

Importantly, our disinfectant solution suggested a complete inactivation of the H5N1 virus activity, as non-hemagglutination was detected. It is essential to highlight that H5N1 avian influenza shares an enveloped structure that conserves stability against different chemical and environmental conditions.<sup>55,56</sup> Thus, illustrating similar trends of viral behavior such as SARS-CoV-2. Therefore, considering that the H5N1 highly pathogenic pandemic strain was inactivated using our nano-formulation, we can firmly state that our decontamination process will give confidence in an appropriate safety margin for sufficient SARS-CoV-2 inactivation and additional benefits of disinfecting other viral pathogens.

Due to the information we recollected, this work presents the performance of an affordable, simple method for the formulation and impregnation of a nano-disinfectant within surgical masks. This novel strategy will provide an outstanding effort to decontaminate and reuse surgical masks in clinical environments, as an endeavor to attend to the current shortage of the supply chain. Moreover, we believe that the insertion of AgNPs will significantly reduce the transmission of broad-spectrum pathogens, thanks to the viral-off activity demonstrated here. Our novel method could be extended for N95 respirators and different medical grade textiles; however, more studies to demonstrate improved effectiveness are under work.

## Conclusion

The current outbreak-associated with the SARS-CoV-2 transmission has resulted in an alarming increment of COVID-19 cases. Moreover, a countering side-effect that is facing the healthcare staff has been the shortage in the supply chain regarding the minimal protective equipment. Therefore, in the present study, we developed a new nano-formulation intended to promote antimicrobial activity into surgical mask fibers by impregnating AgNPs as a safety increasing factor. Our nano-disinfectant application resulted in a firm and controlled impregnation of AgNPs without illustrating fiber alterations, suggesting conserved filtration effectiveness. Far more attractive, our results communicate an extensive antimicrobial activity against secondary associated COVID-19 bacterial infections and *C. albicans*, a problematic nosocomial opportunistic yeast. Moreover, the antiviral efficiency of

our nano-disinfectant showed effective viral inactivation outcomes against H5N1, a pandemic enveloped surrogate of SARS-CoV-2. A significant step forward was the effective antimicrobial action of the impregnated fibers, suggesting a substantial shielding by the AgNPs impregnation. Given the importance of engineering the personnel protective equipment, the present work brings an affordable, effective, and integrated approach for improving the reuse of surgical masks. Likewise, our contribution has potential applications for N95 respirators and different clinical textile materials.

## Acknowledgments

The authors wish to thank the program No. A1-S-38368, “Proyecto Apoyado por el Fondo Sectorial de Investigación para la Educación” CB2017-2018, SEP-CONACYT, for financial support. The authors also acknowledge Dr Minerva Guerra-Balcazar for her valuable support for the XRD analysis and interpretations.

## Author Contributions

All authors made substantial contributions to conception and design, acquisition of data, or analysis and interpretation of data; took part in drafting the article or revising it critically for important intellectual content; agreed to submit to the current journal; gave final approval of the version to be published; and agree to be accountable for all aspects of the work.

## Disclosure

Dr Benjamin Valdez-Salas and Dr Ernesto Beltran-Partida report grants from Consejo Nacional De Ciencia Y Tecnologia, during the conduct of the study. The authors declare no other competing interest regarding the publication of this work.

## References

1. Sun P, Qie S, Liu Z, Ren J, Li K, Xi J. Clinical characteristics of hospitalized patients with SARS-CoV-2 infection: a single arm meta-analysis. *J Med Virol.* 2020;92(6):612–617. doi:10.1002/jmv.25735
2. Wang L, Didelot X, Yang J, et al. Inference of person-to-person transmission of COVID-19 reveals hidden super-spreading events during the early outbreak phase. *Nat Commun.* 2020;11(1):5006. doi:10.1038/s41467-020-18836-4
3. Salehi M, Ahmadikia K, Badali H, Khodavaisy S. Opportunistic fungal infections in the epidemic area of COVID-19: a clinical and diagnostic perspective from Iran. *Mycopathologia.* 2020;185(4):607–611.

4. Lansbury L, Lim B, Baskaran V, Lim WS. Co-infections in people with COVID-19: a systematic review and meta-analysis. *J Infect.* 2020;81(2):266–275. doi:10.1016/j.jinf.2020.05.046
5. Manohar P, Loh B, Nachimuthu R, Hua X, Welburn SC, Leptihn S. Secondary bacterial infections in patients with viral pneumonia. *Front Med.* 2020;7:420. doi:10.3389/fmed.2020.00420
6. Eikenberry SE, Mancuso M, Iboi E, et al. To mask or not to mask: modeling the potential for face mask use by the general public to curtail the COVID-19 pandemic. *Infect Dis Model.* 2020;5:293–308. doi:10.1016/j.idm.2020.04.001
7. Chu DK, Akl EA, Duda S, et al. Physical distancing, face masks, and eye protection to prevent person-to-person transmission of SARS-CoV-2 and COVID-19: a systematic review and meta-analysis. *Lancet.* 2020;395(10242):1973–1987. doi:10.1016/S0140-6736(20)31142-9
8. Bartoszko JJ, Farooqi MAM, Alhazzani W, Loeb M. Medical masks vs N95 respirators for preventing COVID-19 in healthcare workers: a systematic review and meta-analysis of randomized trials. *Influenza Other Respi Viruses.* 2020;14(4):365–373. doi:10.1111/irv.12745
9. Pascarella G, Strumia A, Piliago C, et al. COVID-19 diagnosis and management: a comprehensive review. *J Intern Med.* 2020;288(2):192–206. doi:10.1111/joim.13091
10. Pascoe MJ, Robertson A, Crayford A, et al. Dry heat and microwave-generated steam protocols for the rapid decontamination of respiratory personal protective equipment in response to COVID-19-related shortages. *J Hosp Infect.* 2020;106(1):10–19. doi:10.1016/j.jhin.2020.07.008
11. Zulauf KE, Green AB, Nguyen Ba AN, et al. Microwave-generated steam decontamination of N95 respirators utilizing universally accessible materials. *mBio.* 2020;11(3):e00997–00920. doi:10.1128/mBio.00997-20
12. Cheng VCC, Wong SC, Kwan GSW, Hui WT, Yuen KY. Disinfection of N95 respirators by ionized hydrogen peroxide during pandemic coronavirus disease 2019 (COVID-19) due to SARS-CoV-2. *J Hosp Infect.* 2020;105(2):358–359. doi:10.1016/j.jhin.2020.04.003
13. Talebian S, Wallace GG, Schroeder A, Stellacci F, Conde J. Nanotechnology-based disinfectants and sensors for SARS-CoV-2. *Nat Nanotechnol.* 2020;15(8):618–621. doi:10.1038/s41565-020-0751-0
14. Sportelli MC, Izzi M, Kukushkina EA, et al. Can nanotechnology and materials science help the fight against SARS-CoV-2? *Nanomaterials.* 2020;10(4):802. doi:10.3390/nano10040802
15. Ma Z, Liu J, Liu Y, Zheng X, Tang K. Green synthesis of silver nanoparticles using soluble soybean polysaccharide and their application in antibacterial coatings. *Int J Biol Macromol.* 2021;166:567–577. doi:10.1016/j.ijbiomac.2020.10.214
16. Liu X, Shan K, Shao X, et al. Nanotoxic effects of silver nanoparticles on normal HEK-293 cells in comparison to cancerous HeLa cell line. *Int J Nanomedicine.* 2021;16:753–761. doi:10.2147/IJN.S289008
17. Koyappayil A, Lee M-H. Ultrasensitive materials for electrochemical biosensor labels. *Sensors.* 2021;21(1):89. doi:10.3390/s21010089
18. Li Y, Leung P, Yao L, Song QW, Newton E. Antimicrobial effect of surgical masks coated with nanoparticles. *J Hosp Infect.* 2006;62(1):58–63. doi:10.1016/j.jhin.2005.04.015
19. Huang Z, Jiang H, Liu P, et al. Continuous synthesis of size-tunable silver nanoparticles by a green electrolysis method and multi-electrode design for high yield. *J Mater Chem A.* 2015;3(5):1925–1929. doi:10.1039/C4TA06782G
20. Khaydarov RA, Khaydarov RR, Gapurova O, Estrin Y, Schepel T. Electrochemical method for the synthesis of silver nanoparticles. *J Nanoparticle Res.* 2009;11(5):1193–1200. doi:10.1007/s11051-008-9513-x
21. Valdez-Salas B, Beltrán-Partida E, Nedev N, et al. Controlled antifungal behavior on Ti6Al4V nanostructured by chemical nanopatterning. *Mater Sci Eng C.* 2019;96:677–683. doi:10.1016/j.msec.2018.11.086
22. Ma W, Li Y, Gao S, et al. Self-healing and superwetable nanofibrous membranes with excellent stability toward multifunctional applications in water purification. *ACS Appl Mater Interfaces.* 2020;12(20):23644–23654. doi:10.1021/acsami.0c05701
23. Ma W, Li Y, Zhang M, et al. Biomimetic durable multifunctional self-cleaning nanofibrous membrane with outstanding oil/water separation, photodegradation of organic contaminants, and antibacterial performances. *ACS Appl Mater Interfaces.* 2020;12(31):34999–35010. doi:10.1021/acsami.0c09059
24. Beighton D, Ludford R, Clark DT, et al. Use of CHROMagar Candida medium for isolation of yeasts from dental samples. *J Clin Microbiol.* 1995;33(11):3025. doi:10.1128/JCM.33.11.3025-3027.1995
25. Valdez-Salas B, Beltrán-Partida E, Zlatev R, et al. Structure-activity relationship of diameter controlled Ag@Cu nanoparticles in broad-spectrum antibacterial mechanism. *Mater Sci Eng C.* 2021;119:111501. doi:10.1016/j.msec.2020.111501
26. Dey BP, Engley FB. Neutralization of antimicrobial chemicals by recovery media. *J Microbiol Methods.* 1994;19(1):51–58. doi:10.1016/0167-7012(94)90025-6
27. Secretaría de Economía, Diario Oficial de la Federación N-B-S. General methods for analysis of antimicrobial activity. Determination of germicidal activity. Norma Oficial Mexicana. 1999.
28. Eisfeld AJ, Neumann G, Kawaoka Y. Influenza A virus isolation, culture and identification. *Nat Protoc.* 2014;9(11):2663–2681. doi:10.1038/nprot.2014.180
29. Beltrán-Partida E, Valdez-Salas B, Valdez-Salas E, Pérez-Cortéz G, Nedev N. Synthesis, characterization, and in situ antifungal and cytotoxicity evaluation of ascorbic acid-capped copper nanoparticles. *J Nanomater.* 2019;2019:5287632. doi:10.1155/2019/5287632
30. Glover RD, Miller JM, Hutchison JE. Generation of metal nanoparticles from silver and copper objects: nanoparticle dynamics on surfaces and potential sources of nanoparticles in the environment. *ACS Nano.* 2011;5(11):8950–8957. doi:10.1021/nn2031319
31. Garcia PRAF, Prymak O, Grasmik V, et al. An in situ SAXS investigation of the formation of silver nanoparticles and bimetallic silver-gold nanoparticles in controlled wet-chemical reduction synthesis. *Nanoscale Adv.* 2020;2(1):225–238. doi:10.1039/C9NA00569B
32. Wang H, Qiao X, Chen J, Wang X, Ding S. Mechanisms of PVP in the preparation of silver nanoparticles. *Mater Chem Phys.* 2005;94(2):449–453. doi:10.1016/j.matchemphys.2005.05.005
33. Badawy AME, Luxton TP, Silva RG, Scheckel KG, Suidan MT, Tolaymat TM. Impact of environmental conditions (pH, ionic strength, and electrolyte type) on the surface charge and aggregation of silver nanoparticles suspensions. *Environ Sci Technol.* 2010;44(4):1260–1266. doi:10.1021/es902240k
34. Barani H. Surface activation of cotton fiber by seeding silver nanoparticles and in situ synthesizing ZnO nanoparticles. *New J Chem.* 2014;38(9):4365–4370. doi:10.1039/C4NJ00547C
35. Osório I, Igreja R, Franco R, Cortez J. Incorporation of silver nanoparticles on textile materials by an aqueous procedure. *Mater Lett.* 2012;75:200–203. doi:10.1016/j.matlet.2012.02.024
36. Li X, Lenhart JJ, Walker HW. Dissolution-accompanied aggregation kinetics of silver nanoparticles. *Langmuir.* 2010;26(22):16690–16698. doi:10.1021/la101768n
37. Hiragond CB, Kshirsagar AS, Dhapte VV, Khanna T, Joshi P, More PV. Enhanced anti-microbial response of commercial face mask using colloidal silver nanoparticles. *Vacuum.* 2018;156:475–482. doi:10.1016/j.vacuum.2018.08.007
38. Kowalczyk D, Kaminska I. Effect of pH and surfactants on the electrokinetic properties of nanoparticles dispersions and their application to the PET fibres modification. *J Mol Liq.* 2020;320:114426. doi:10.1016/j.molliq.2020.114426
39. Chamakura K, Perez-Ballesteros R, Luo Z, Bashir S, Liu J. Comparison of bactericidal activities of silver nanoparticles with common chemical disinfectants. *Colloids Surf B Biointerfaces.* 2011;84(1):88–96. doi:10.1016/j.colsurfb.2010.12.020

40. Cheikhrouhou W, Ferrara AM, Botelho Do Rego AM, Ferreira Machado I, Vieira Ferreira LF, Boufi S. Cotton fabrics decorated with nanostructured Ag/AgX (X:Cl,Br) as reusable solar light-mediated bactericides: a comparative study. *Colloids Surf B Biointerfaces*. 2020;196:111342. doi:10.1016/j.colsurfb.2020.111342
41. Li C, Wang X, Chen F, et al. The antifungal activity of graphene oxide-silver nanocomposites. *Biomaterials*. 2013;34(15):3882–3890. doi:10.1016/j.biomaterials.2013.02.001
42. Zhao Z, Zhang Z, Lanzarini-Lopes M, et al. Germicidal ultraviolet light does not damage or impede performance of N95 masks upon multiple uses. *Environ Sci Technol Lett*. 2020;7(8):600–605. doi:10.1021/acs.estlett.0c00416
43. Fischer R, Morris D, van Doremalen N, et al. Effectiveness of N95 respirator decontamination and reuse against SARS-CoV-2 virus. *Emerg Infect Dis*. 2020;26(9):2253. doi:10.3201/eid2609.201524
44. Liao L, Xiao W, Zhao M, et al. Can N95 respirators be reused after disinfection? How many times? *ACS Nano*. 2020;14(5):6348–6356. doi:10.1021/acsnano.0c03597
45. Cui J, Lu T, Li F, et al. Flexible and transparent composite nanofibre membrane that was fabricated via a “green” electrospinning method for efficient particulate matter 2.5 capture. *J Colloid Interface Sci*. 2021;582:506–514. doi:10.1016/j.jcis.2020.08.075
46. van Doremalen N, Bushmaker T, Morris DH, et al. Aerosol and surface stability of SARS-CoV-2 as compared with SARS-CoV-1. *N Engl J Med*. 2020;382(16):1564–1567. doi:10.1056/NEJMc2004973
47. Chan KH, Sridhar S, Zhang RR, et al. Factors affecting stability and infectivity of SARS-CoV-2. *J Hosp Infect*. 2020;106(2):226–231. doi:10.1016/j.jhin.2020.07.009
48. Kampf G, Todt D, Pfaender S, Steinmann E. Persistence of coronaviruses on inanimate surfaces and their inactivation with biocidal agents. *J Hosp Infect*. 2020;104(3):246–251. doi:10.1016/j.jhin.2020.01.022
49. Furno F, Morley KS, Wong B, et al. Silver nanoparticles and polymeric medical devices: a new approach to prevention of infection? *J Antimicrob Chemother*. 2004;54(6):1019–1024. doi:10.1093/jac/dkh478
50. Palmieri V, Papi M. Can graphene take part in the fight against COVID-19? *Nano Today*. 2020;33:100883. doi:10.1016/j.nantod.2020.100883
51. AshaRani PV, Low Kah Mun G, Hande MP, Valiyaveetil S. Cytotoxicity and genotoxicity of silver nanoparticles in human cells. *ACS Nano*. 2009;3(2):279–290. doi:10.1021/nn800596w
52. Park MVDZ, Neigh AM, Vermeulen JP, et al. The effect of particle size on the cytotoxicity, inflammation, developmental toxicity and genotoxicity of silver nanoparticles. *Biomaterials*. 2011;32(36):9810–9817. doi:10.1016/j.biomaterials.2011.08.085
53. Sweet MJ, Singleton I. Soil contamination with silver nanoparticles reduces bishop pine growth and ectomycorrhizal diversity on pine roots. *J Nanoparticle Res*. 2015;17(11):448. doi:10.1007/s11051-015-3246-4
54. Yan A, Chen Z. Impacts of silver nanoparticles on plants: a focus on the phytotoxicity and underlying mechanism. *Int J Mol Sci*. 2019;20(5):1003. doi:10.3390/ijms20051003
55. Otter JA, Donskey C, Yezli S, Douthwaite S, Goldenberg SD, Weber DJ. Transmission of SARS and MERS coronaviruses and influenza virus in healthcare settings: the possible role of dry surface contamination. *J Hosp Infect*. 2016;92(3):235–250. doi:10.1016/j.jhin.2015.08.027
56. Figueroa A, Hauck R, Saldias-Rodriguez J, Gallardo RA. Combination of quaternary ammonia and glutaraldehyde as a disinfectant against enveloped and non-enveloped viruses. *J Appl Poult Res*. 2017;26(4):491–497. doi:10.3382/japr/pfx021

## International Journal of Nanomedicine

### Publish your work in this journal

The International Journal of Nanomedicine is an international, peer-reviewed journal focusing on the application of nanotechnology in diagnostics, therapeutics, and drug delivery systems throughout the biomedical field. This journal is indexed on PubMed Central, MedLine, CAS, SciSearch®, Current Contents®/Clinical Medicine,

Journal Citation Reports/Science Edition, EMBase, Scopus and the Elsevier Bibliographic databases. The manuscript management system is completely online and includes a very quick and fair peer-review system, which is all easy to use. Visit <http://www.dovepress.com/testimonials.php> to read real quotes from published authors.

Submit your manuscript here: <https://www.dovepress.com/international-journal-of-nanomedicine-journal>

Dovepress